

Gas molecules (CO, NH₃, CO₂) sensing with Polyaniline Emeraldine salt (PANI ES) : a turbo TDDFT study

N. Hadian Jazi^a, I. Abdolhosseini Sarsari^{b,c}, and N. Zare Dehnavi^a

^aDepartment of Physics, Central Tehran Branch, Islamic Azad University, Tehran, Iran

^bDepartment of Physics, Isfahan University of Technology, Isfahan, 84156-83111, Iran

^cComputational Physical Sciences Research Laboratory, School of Nano-Science, Institute for Research in Fundamental Sciences (IPM), P.O. Box 19395-5531, Tehran, Iran

(Dated: October 1, 2018)

The adsorption of gas molecules (CO, NH₃, CO₂) on Polyaniline Emeraldine salt has been performed to study gas sensing. Density functional theory (DFT) and time dependent density functional theory (TD-DFT) calculations have been carried out to compute the response mechanism of polyaniline emeraldine salt (PANI ES) oligoanilines (with two to six rings) to gas molecules. The optimized geometry and electronic structure corresponding to molecule and complexes are computed with the pseudo-potential and full-potential methods. The absorption spectra corresponding to polyaniline emeraldine salt molecule and its complexes are calculated using TD-DFT. We found it out that the electronic and optical features corresponding to complexes show more sensitive to the NH₃ adsorption. The optical absorption spectrum analysis was used for all (nPANI ES-X) and isolated nPANI ES. Then, the related spectrum indicates that the λ_{max} is shifted red or blue, is affected by the kind of complex.

I. INTRODUCTION

Some gas molecules such as CO, NH₃, CO₂ can make serious problems, therefore their detection at ppm and/or ppb concentration is so important for the human safety and health¹⁻⁵. Many articles recently gave emphasis to property of gas sensors. In the last few years, a new generation of gas sensors has been prepared, using conductive polymers (CP)⁶⁻⁸. It is found that the conductive polymers could be utilized for detecting small concentration of CO, NH₃, CO₂ with high sensitivity at ambient temperature⁹.

Conductive polymers (CPs) (Polyaniline (PANI), polypyrrole (PPY), poly(o-phenylenediamine) (POPD) and poly(3,4-ethylenedioxythiophene) (PEDOT)) have received a lot of attention since the first discovery of polyacetylen (CH)_x in 1977^{10,11}. The many single subject studies demonstrate their biosensing and gas sensing capabilities⁶.

Among CPs, PANI was studied as gas sensors, experimentally and theoretically. People hope they will profit greatly from its low cost, high sensitivity, environmental stability and short response time toward guest molecule at ambient temperature in sensing devices^{12,13}. The response mechanisms of PANI to gas molecules were studied theoretically to give some explanations for empirical observations in detail¹⁴⁻¹⁶. Recently, more and more theoretical papers have been published concerning PANI by the mean of Ab-initio or density functional theory (DFT) methods¹⁷⁻²⁰. Geometric and electronic structures of various neutral aniline oligomers were studied by Lim et al²¹.

In this paper, we studied a variety of complexes to model the interaction between individual oligoanilines and different gas molecules with (DFT) and Time-Dependent Density Functional Theory (TD-DFT) approaches. Based on the synthesis procedure, PANI has

three different oxidation states: PANI Lecuemeraldin base (LB), Pernigraniline base (PNB), Emeradin base (EB). Acid doping, nitrogen in PANI-EB chain is able to be protonated to afford conducting Emeraldine salt (ES) which indicates excellent conductivity as the result of extensive π conjugating in the polymer chain²². In this work, we mainly investigated electronic, optical and structural PANI ES, and the effect of interacted gas molecules on it. Radical cation ES oligoanilines with two, four and six benzene rings ended by nitrogen atoms are represented in Fig. 1.

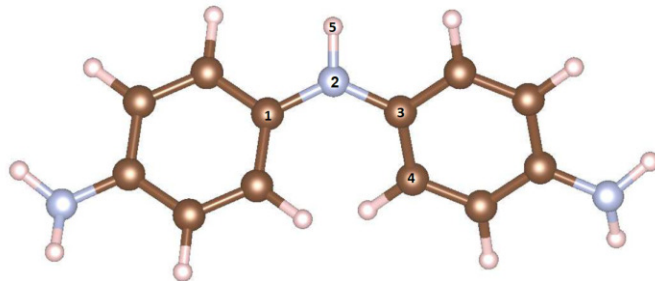


FIG. 1. Optimized structure of PANI ES molecule. The C, N and H atoms indicate with brown, blue and pink spheres respectively.

The general reaction mechanism through which PANI ES gives response to samples X (X=NH₃, CO₂, CO) are given based on the subsequent reactions:



II. COMPUTATIONAL DETAILS

Our electronic structure computation and geometry optimizations have been carried out in the frame-work of (DFT) by using PAW pseudopotential as well as numerical orbital atoms (NAO) full potential methods applied in the Quantum Espresso (QE)²³ and FHI-aims²⁴ computational packages, respectively. GGA-PBE exchange-correlation functionals²⁵ and supercell approach were applied for simulating isolated PANI ES molecule in QE. A vacuum thickness of around 24 Bohr was used for avoiding interaction of neighboring molecules. Cut-off energy of 40 Ry and 500 Ry, is applied for plane wave development of wave functions and electron density, However full potential computations were carried out with *tier3* base set and atomic ZORA scalar relativistic impacts.

Electronic properties the energy of the highest occupied molecular orbital (E_{HOMO}), the energy of the lowest unoccupied molecular orbital (E_{LUMO}) and HL gap (E_{HL}) are calculated at the previously mentioned level of the theory. The chemical potential (μ) was defined via²⁶.

$$\mu = \frac{-(E_{HOMO} + E_{LUMO})}{2} \quad (3)$$

In addition, the hardness η can be calculated by the use of Koopmans theorem as:

$$\eta = \frac{(E_{LUMO} - E_{HOMO})}{2} \quad (4)$$

Softness (S) was described using the following equations²⁷:

$$S = \frac{1}{2\eta} \quad (5)$$

To compute the gas molecules adsorption energy on nPANI ES, Equation (5) has been used.

$$E_{ads} = E_{nPANIES-x} - (E_{nPANIES} + E_X). \quad (6)$$

where $E_{nPANIES-x}$ is the whole energy of the optimized nPANI ES interacted with diverse molecules of gas, $E_{nPANIES}$ is the throughout energy of an isolated nPANI ES, E_X is the full energy of any gas molecules in the relaxed form.

The optical absorption spectrum of the molecules is calculated in the framework of Liouville-Lanczos approach to time-dependent DFT, implemented in Turbo-TDDFT code, that is part of QE distribution^{28,29}. The Liouville-Lanczos approach iterations optimized 2000 for our calculations.

III. RESULTS AND DISCUSIONS

The interaction of NH₃, CO₂, CO gas molecules with PANI ES on different positions have been optimized using the above mentioned method. For NH₃ and CO₂, just

one configuration on PANI ES can be optimized, However two configurations can be optimized for CO (O end and C end) nPANI ES-OC (CO(1)) and nPANI ES-CO (CO(2)). Following complete optimization of all configurations on PANI ES, the most stable one was applied for further the study. We find that the divers gas molecules prefer different geometries in the adsorption. Our data of the optimized geometric parameters and the data of the absorption energy are listed in tableI. The geometries of the optimized complexes deliver important data about the response mechanism of conduction toward different gas molecules.

The distance between H5 and X gas ($d_{H5..X}$) shows notable changes in different gas molecules adsorption. The nearest distance between nPANI ES and gas molecules is confirmed for NH₃ by the distance of 1.87Å, 1.84Å, 1.84 Å for n=2,4,6, respectively, which points to strong interaction between them but CO(1) and CO(2) have the largest distance which points to less interaction between them. This result is completely in agreement with the obtained adsorption energies. For nPANI ES-NH₃ complexes, $d_{H5..X}$ distance decreases about 0.03Å from 2 to 6. The reduction of $d_{H5..X}$ distance with chain length elongation illustrates the reduction in interaction with chain elongation. The distance $d_{N2..H5}$ increases when nPANI ES interacts with ammonia (table I). This bond enhance/reduce as the result of generating/losing of ion dipole electrostatic interaction between nPANI ES and the above-mentioned molecules.

Another important geometric factor in nPANI ES and nPANI ES-X is the bridging angle ($\angle C_1N_2C_3$) which decrease when nPANI ES interacts with NH₃ molecule. The maximum and minimum decrease in angle is about 2.07 Å and 1.1 Å in 4PANI ES-NH₃ and 6PANI ES-CO(1) complexes regarding their equivalent non-complexed nPANI ES. The larger decrease in angle means the stronger electrostatic attraction between nPANI ES and NH₃. considering the analysis of the decrease in bond angles, it can be concluded that the interaction between nPANI ES and NH₃ increase and alongside the increase in chain length elongation, consistent with the inference from the bond length analysis (vide supra).

Another important parameter is the $\angle N_2H_5..X$ angle which only shows the situation of gas molecules on nPANI ES. it increases from about 129 degree (in nPANI ES) to about 180 degree in all nPANI ES-X complexes. As the result of existing different gas molecules which is presented in table I the dihedral angle $\angle C_1N_2C_3C_4$ is altered based on the kind of X as guests which are possibly beacuse of the ion dipole interaction. This factor will influence the electronic structure of complexes.

A. Electronic properties

The electronic structure corresponding to the best nPANI ES molecule and its complexes were computed with both pseudo-potential and full potential methods

TABLE I. Optimized geometric of parameters using DFT level of theory (Bond lengths in Å, bond angles in deg).

Species	$d_{H5...X}(vdw)$	$d_{N2...H5}$	$\angle C_1N_2C_3$	$\angle N_2H_5...X$	$\angle C_1N_2C_3C_4$
Isolated 2PANI ES	-	1.01	129.04	-	22.27
2PANI ES-CO(2)	2.19	1.01	129.01	179.75	22.29
2PANI ES-CO(1)	2.12	1.02	128.58	179.91	23.07
2PANI ES-CO ₂	2.07	1.01	129.16	179.98	21.86
2PANI ES-NH ₃	1.87	1.04	127.71	179.29	24.49
Isolated 4PANI ES	-	1.01	130.36	-	22.58
4PANI ES-CO(2)	2.12	1.02	129.02	179.25	22.67
4PANI ES-CO(1)	2.12	1.01	129.04	179.15	22.35
4PANI ES-CO ₂	2.00	1.01	129.57	179.78	20.97
4PANI ES-NH ₃	1.84	1.04	128.29	178.66	23.04
Isolated 6PANI ES	-	1.01	129.53	-	21.65
6PANI ES-CO(2)	2.08	1.01	129.50	179.82	20.78
6PANI ES-CO(1)	2.13	1.02	128.95	179.78	22.13
6PANI ES-CO ₂	1.99	1.01	129.53	179.68	21.44
6PANI ES-NH ₃	1.84	1.04	128.43	177.83	23.28

and result showed an excellent was observed. The electronic properties of nPANI ES are completely modified by gas molecules. The prime focus of the present work is on ionization electron, electron affinity, HOMO-LUMO(HL) gap and adsorption characteristic of gas molecules on nPANI ES. Table II represents the HOMO energy, LUMO energy, Dipole moment, Mulliken charge transfer, HL gap and adsorption energy of isolated nPANI ES and nPANI ES complexes. The HL gap of isolated nPANI ES is 2.71, 2.31 and 2.36 eV for n=2, 4, 6.

The incorporation of gas molecules decreases the E_{HL} except for 4PANI ES-NH₃. So we conclude that for n =2-6 the highest conductivity between nPANI ES and different gas molecules are confirmed for CO(1), CO(2). Analyzing the HL gap variation upon gas molecules adsorption on nPANI ES isolated clearly suggests that nPANI ES can be used as a sensor. As can be observed in table II, the HL gap of each gas molecules is much higher than the HL gap of nPANI ES.

However, upon complexation, the HL gap of the resultant complex is quite different from that one for of the nPANI ES, depending on the nature of the gas molecules. It can be said (but it is not true for all cases) that the smaller difference in the HL gap of gas molecules and nPANI ES molecule, the greater change in HL gap of their complex (further hybridization), and as it can be observed for CO(2), CO(1). For other samples like CO₂ the large difference in the E_{HL} of the gas molecule and nPANI ES results in an inconsiderable variation in the HL gap of the resultant complex, which makes it difficult to transfer electrons³⁰.

When gas molecules get adsorbed on nPANI ES, the alteration in adsorption energy would be observed. The positive and negative values of E_{ad} show the endothermic and exothermic reaction respectively, based on the adsorption of gas molecules on nPANI ES. The adsorption energy magnitude is different and a negative value of adsorption energy infers that the energy transfers from

isolated nPANI ES to gas molecules. The adsorption energy magnitude for nPANI ES-NH₃ is higher than others.

The electronic features can also be discussed in terms of Mulliken charge transfer (Q) between gas molecules and isolated nPANI ES. The positive value corresponding to Mulliken charge transfer indicates the charge transfer from gas molecules to nPANI ES, while the negative value corresponding to Mulliken charge transfer indicates the charge transfer from nPANI ES isolated to gas molecules. In the present work, for all positions, the positive value of Mulliken charge transfer is taken in to consideration and indicates the electrons transfer from gas molecules to nPANI ES. The magnitude of Mulliken charge transfer is found to be higher when NH₃ molecule get adsorbed on nPANI ES comparing to the adsorption of other molecules and it is due to more value of adsorption energy for nPANI ES-NH₃ that can be observed in table II.

A weak interaction is observed in nPANI ES-CO₂ complexes, comparing those of nPANI ES-NH₃ (see table II). The HOMO of 2PANI ES gets electric charge clouds from CO₂ of nearby 0.13 eV which is 0.2 eV smaller comparing to that of the 2PANI ES-NH₃ complex. The transfer of this electron clouds happen from the HOMO of CO₂ to LUMO of nPANI ES, instead of ion-dipole electrostatic interaction with ammonia, give a rise to a weak type of attractive force. The small electron cloud transfer from analyte to polymer in 2PANI ES-CO₂ comparing to 2PANI ES-NH₃ complex manifests itself in weak sensing of CO₂ using the polymer. The 4PANI ES-CO₂ and 6PANI ES-CO₂ complexes have 0.17 eV and 0.03 eV smaller electron cloud attraction, respectively, as comparing to its nPANI ES-NH₃.

The computed amounts of dipole moment μ_D of interacted CO(1), CO(2), CO₂ and NH₃ with nPANI ES are presented in table II³¹. The dipole moment considers the electronic and geometrical features and gives an insight into the distribution of charges in alone Polyaniline emardline salt. Our findings indicated that upon inter-

TABLE II. The calculated electronic properties of nPANI ES and nPANI ES-X complexes, where n = 2-6 and X = NH₃, CO(1), CO(2) and CO₂, $E_g = |E_{HOMO} - E_{LUMO}|$, E_d : adsorption energy, $Q(e)$: Mulliken charge transfer, μ_D : dipole moment.

Species	$E_{HOMO}(eV)$	$E_{LUMO}(eV)$	$E_{HL}(eV)$	$E_{ad}(eV)$	$Q(e)$	$\mu_D(Debye)$
Isolated 2PANI ES	-3.69	-0.97	2.72	-	-	-0.22
2PANI ES-CO(2)	-3.63	-2.50	1.12	-0.08	0.02	-0.39
2PANI ES-CO(1)	-3.60	-2.59	1.00	-0.16	0.03	-0.60
2PANI ES-CO ₂	-3.56	-1.15	2.41	-0.12	0.01	-0.90
2PANI ES-NH ₃	-3.36	-0.95	2.41	-0.41	0.06	-3.00
Isolated 4PANI ES	-3.39	-1.07	2.31	-	-	24.76
4PANI ES-CO(2)	-3.41	-2.47	0.93	-0.17	0.03	27.22
4PANI ES-CO(1)	-3.42	-2.39	1.03	-0.08	0.02	27.82
4PANI ES-CO ₂	-3.37	-1.06	2.31	-0.13	0.01	31.80
4PANI ES-NH ₃	-3.23	-0.89	2.34	-0.43	0.06	32.67
Isolated 6PANI ES	-3.35	-0.98	2.36	-	-	-1.11
6PANI ES-CO(2)	-3.37	-2.41	0.95	-0.08	0.02	23.59
6PANI ES-CO(1)	-3.36	-2.49	0.87	-0.17	0.03	22.04
6PANI ES-CO ₂	-3.33	-1.07	2.25	-0.13	0.02	22.59
6PANI ES-NH ₃	-3.22	-0.97	2.25	-0.50	0.06	25.29
CO(2)	-9.11	-2.32	6.78	-	-	0.16
CO(1)	-9.10	-2.31	6.79	-	-	-0.17
CO ₂	-9.34	-1.01	8.32	-	-	-0.01
NH ₃	-6.12	-0.74	5.38	-	-	-1.37

action of analytes with nPANI ES the dimension and directions of μ_D will be changed based on the configuration of adsorption. As presented in table II, for each system of interaction with nPANI ES, the dipole moment increased compare to isolated nPANI ES.

Orbital density of nPANI ES molecule and several of its derivatives are computed and showed in table III. The main activity of electrons is in the state of HOMO. Therefor we are pretty zealous to study the HOMO-LUMO orbitals of all structures. As it is presented in table III. The distribution of HOMO and LUMO (See table III) for nPANI ES and complexed forms of species are: nPANI ES-CO(2), nPANI ES-CO(1), nPANI ES-CO₂ and nPANI ES-NH₃ for (n=2,4,6). As can be seen in table III for all systems, HOMO is localized on nPANI ES molecule except for 4PANI ES-CO(2) and 6PANI ES-CO(1), the HOMO are located on both CO(2), CO(1) and 4PANI ES, 6PANI ES-CO(1). This relocation of HOMO corresponds to the highest change in the E_{HL} and causes the highest interaction energy. Similarly, for 2PANI ES, 4PANI ES and 6PANI ES, 4 PANI ES-CO₂ the LUMO is located on nPANI ES molecule due to weak interaction between nPANI ES with gas molecules. The LUMO for 2PANI ES-CO(2), 2PANI ES-CO(1), 4PANI ES-CO(2), 4PANI ES-CO(1), 6PANI ES-CO(2) and 6PANI ES-CO(1) are thoroughly located on the CO(2), CO(1) with an exception for 2PANI ES-CO₂, 2PANI ES-NH₃, 6PANI ES-CO₂, 4PANI ES-NH₃, the LUMO which are localized both on CO₂, NH₃ and polymer rings. This relocation of LUMO corresponds to the highest change in the E_{HL} , that results in the highest interaction energy.

Table IV represents the global reactivity indices which are computed by DFT for the highest stable configura-

tion of gas molecules adsorbed onto nPANI ES molecule; The electronic features of nPANI ES can also be discussed in terms of Ionization Potential (IP) and Electron Affinity (EA). IP denotes the amount of energy required to remove the electron from nPANI ES. For n=2, high value of IP is observed for isolated nPANI ES, and IP decrease after incorporation of gas molecules but high value of IP for n=4,6 relates to 4PANI ES-CO(1) and 6PANI ES-CO(2). High value of IP infers that the electrons in nPANI ES complexes are bound to the isolated nPANI ES. EA represents the alteration in the energy because of the adding electron in nPANI ES. The high value of EA is one of the favorable conditions for chemical sensors. Since the global hardness of a species is defined as its resistance against deformation in the existence of an electric field, increasing the global hardness increases the stability and reduces the reactivity of the species²⁶. The global electrophilicity includes data on the chemical potential (which is related to electron transfer) and the hardness, (which is related to stability). Note that, for nPANI ES-CO(1) and nPANI ES-CO(2) the HL gap is relatively small, leading to low hardness value for this complex comparing the softness, electrophilicity and electronic chemical potential values which are high. It can be concluded that the enhanced hardness of complexes indicates that they are more stable in good according to the high HL gap recorded for these complexes.

B. Electronic and Vibrational Properties

The electronic structures corresponding to the optimized nPANI ES and nPANI ES-X molecules are calculated by using both pseudo-potential and full poten-

TABLE III. Orbital density of nPANI ES molecule and its derivatives.

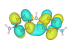
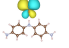
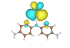
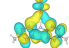
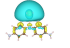
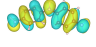
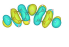

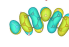

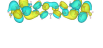
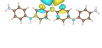
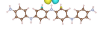
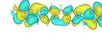



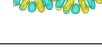
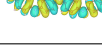
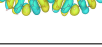
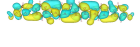
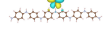
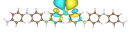
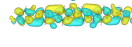


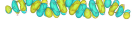



Phase	Isolated 2PANI ES	2PANI ES-CO(2)	2PANI ES-CO(1)	2PANI ES-CO ₂	2PANI ES-NH ₃
LUMO					
HUMO					
Phase	Isolated 4PANI ES	4PANI ES-CO(2)	4PANI ES-CO(1)	4PANI ES-CO ₂	4PANI ES-NH ₃
LUMO					
HUMO					
Phase	Isolated 6PANI ES	6PANI ES-CO(2)	6PANI ES-CO(1)	6PANI ES-CO ₂	6PANI ES-NH ₃
LUMO					
HUMO					

TABLE IV. The global reactivity indices were calculated via DFT for the most stable configuration of NH₃, CO(1), CO(2) and CO₂ adsorbed onto nPANI ES. IP: Ionization potential ($-E_{HOMO}$), EA: electron affinity ($-E_{LUMO}$), η : hardness, μ : chemical potential, S: softness.

Species	IP(eV)	EA(eV)	η (eV)	μ (eV)	S(eV)
2PANI ES	3.69	0.97	1.36	-2.33	0.36
2PANI ES-CO(2)	3.63	2.50	0.56	-3.06	0.88
2PANI ES-CO(1)	3.60	2.59	0.50	-3.09	0.99
2PANI ES-CO ₂	3.56	1.15	1.20	-2.35	0.41
2PANI ES-NH ₃	3.56	0.95	1.30	-2.25	0.38
4PANI ES	3.39	1.07	1.15	-2.23	0.43
4PANI ES-CO(2)	3.41	2.47	0.46	-2.94	1.07
4PANI ES-CO(1)	3.42	2.39	0.51	-2.91	0.96
4PANI ES-CO ₂	3.37	1.06	1.15	-2.22	0.43
4PANI ES-NH ₃	3.23	0.89	1.17	-2.06	0.43
6PANI ES	3.35	0.98	1.18	-2.17	0.42
6PANI ES-CO(2)	3.37	2.41	0.47	-2.89	1.04
6PANI ES-CO(1)	3.36	2.49	0.43	-2.92	1.14
6PANI ES-CO ₂	3.33	1.79	1.13	-2.20	0.45
6PANI ES-NH ₃	3.22	0.97	1.12	-2.09	0.44

tial methodes with a good agreement with each other. The HL gap of 2PANI ES was obtained 2.72 eV within pseudo-potential method, which is significantly bigger than the experimental gap of about 3.48 eV³². This difference shows the major deficiency of LDA/GGA functional for predicting the excited states features. Thus, TD-DFT calculations will be utilized to attain some reliable outcomes for HL gap. The vibrational spectra corresponding to the molecule is computed to study dynamical stability and IR spectrum for the systems. The resulted IR spectrum of the nPANI ES and nPANI ES-X molecules are listed in Fig. 2, Fig. 3 and Fig. 4. Dynam-

ical stability of the molecule proved by the absence of any imaginary style in the spectrum. As an evident, 2PANI ES, 4PANI ES and 6PANI ES have 3 greater IR intensity that relate to the stronger bonds. Vibrations around 598 (cm^{-1}), 1508 (cm^{-1}), 1264 (cm^{-1}), 296 (cm^{-1}), 1506 (cm^{-1}), 1509 (cm^{-1}), 288 (cm^{-1}), 1312 (cm^{-1}) and 1482 (cm^{-1}) frequency show greater IR intensity respectively for 2PANI ES, 4PANI ES and 6PANI ES. We can conclude when rings of PANI ES increased from n=2 to n=6, the value and position of IR intensity, and vibration frequencies are changed.

In addition, when gas molecules get absorbed on nPANI ES, the value of IR intensity and vibrational frequencies are changed. Interaction 2PANI ES-X with gas molecules where X=CO(1), CO(2), CO₂ causes new bonds C=O and O=H around 2120 to 2355 (cm^{-1}) and around 3539 to 3564 (cm^{-1}), respectively. There is also change in the vibrational frequencies position with higher IR intensity in 2PANI ES-X complexes compare to isolated 2PANI ES. The highest amount of C=O bonds IR intensity occurs in nPANI ES-CO₂, while interacting NH₃ with 2PANI ES results in the biggest change in the vibrational frequencies. Similarly, the interaction of 4PANI ES-X and 6PANI ES-X (X=CO(1), CO(2), CO₂) with gas molecules causes new bonds C=O and O=H around 2120 to 2355 (cm^{-1}) and around 3539 to 3564 (cm^{-1}) respectively. We can observe for 2PANI ES-NH₃, 4PANI ES-NH₃ and 6PANI ES-NH₃ the amount of a higher and increased IR intensity. Analyzing the IR spectrum corresponding to the systems with adsorption of gas molecules on an isolated nPANI ES clearly suggests that nPANI ES can be used as sensor.

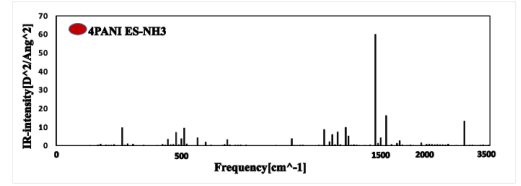
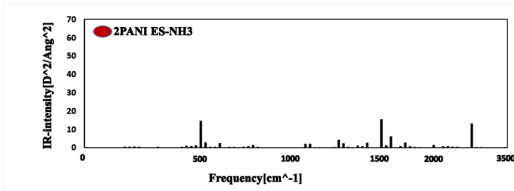
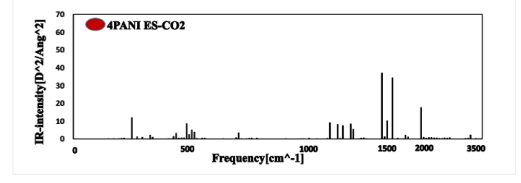
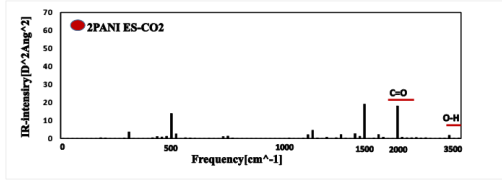
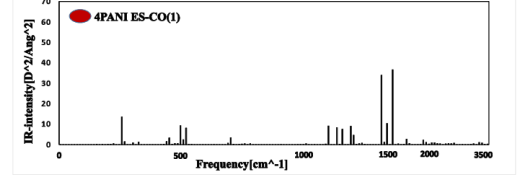
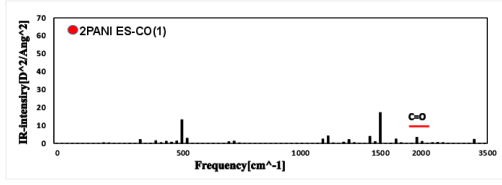
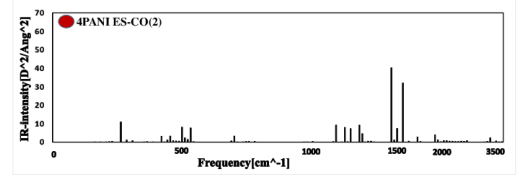
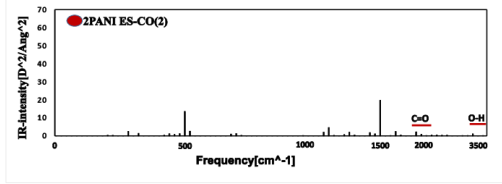
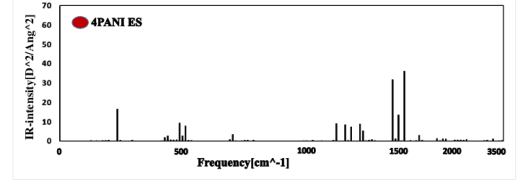
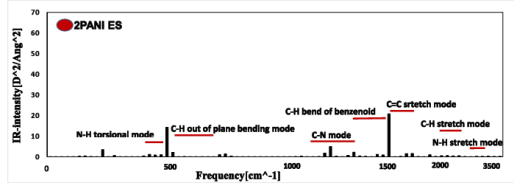


FIG. 2. calculated IR spectrum of 2PANI ES with gas molecules that adsorbed on it.

FIG. 3. calculated IR spectrum of 4PANI ES with gas molecules that adsorbed on it.

C. Optical properties

The Liovile-lanczos approach with TD-DFT is used for determining the optical spectrum. In this method, the

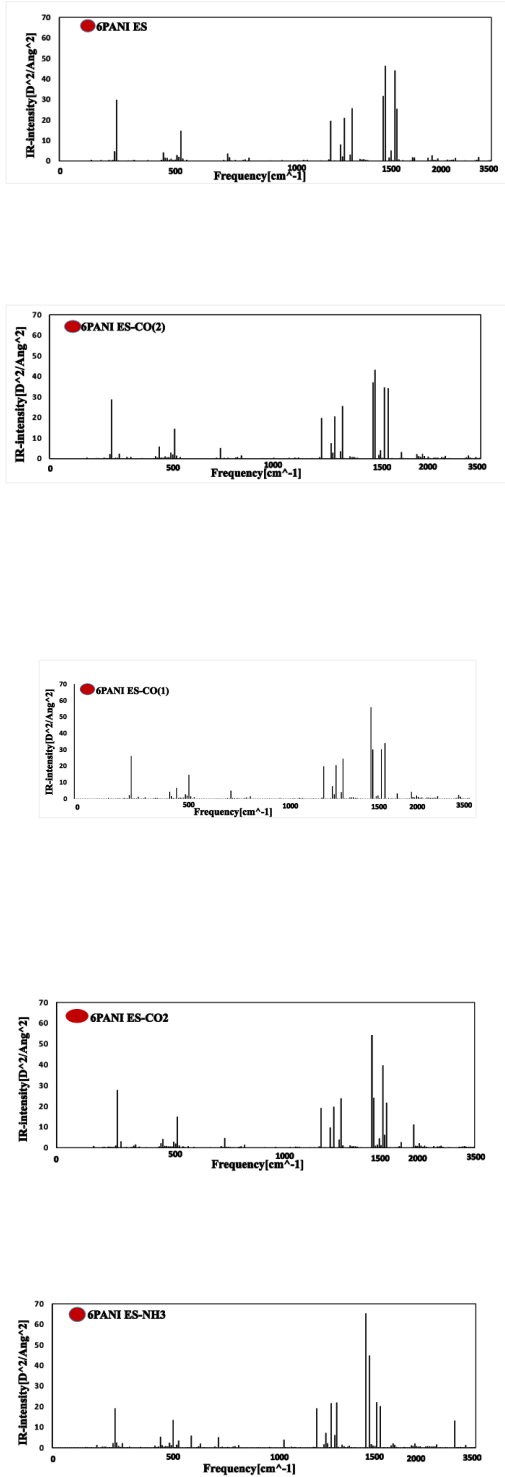


FIG. 4. calculated IR spectrum of 6PANI ES with gas molecules that adsorbed on it.

optimization of iterations number should be performed.

The absorption spectrum corresponding to 2PANI ES have been calculated using various iterations number (Fig. 5). It is observed that a flat optical spectrum is resulted with 1000 iteration, while sharp peaks is observed by enhancing iterations. The obtained absorption spectra with 2000 and 2500 iterations are fully overlapped. Therefore, 2000 iterations is the optimal factor for our following computations.

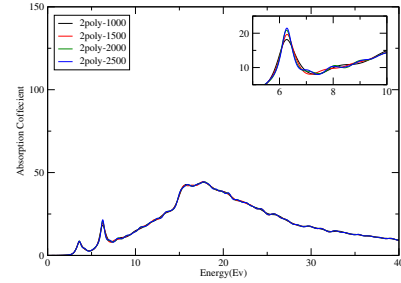


FIG. 5. Optimizing the number of iterations to determine the optical spectrum of the 2PANI ES molecule.

The first peak of the absorption spectrum shows the first excited state and the energy that is equal to the energy needed for transfer of one electron from the (HOMO) to (LUMO). The following peaks in the absorption spectrum represent the subsequent electrons excitation from other states. By enhancing the energy between different states, excitation happens in larger energy. Fig. 6 presents the optical spectrum complexes and the transition states corresponding to nPANI ES molecule. The first peak is just associated with (first excitation), but the following peaks are associated with several excitations which broadening for each peak affecting by the amount of electron excitations in the corresponding energy. The data that are calculated here showed in table V. We used Equation (6) to compute the adsorption energy of gas molecules on nPANI ES.

The experimental λ_{max} value of PANI ES is 356 nm (3.48 eV),³³ which is 0.12 eV lower than our calculated λ_{max} value of 344 nm for free 2PANI ES (3.6 eV). This difference is due to the infinite number of nPANI ES lengths considered in empirical study while our computation simulated is on the basis of the limited length for a polymer having only two, four and six rings.

Obviously, from the data listed in table V, when gas molecules interacts with nPANI ES, the values for complexes are blue-shifted for 2PANI ES and its complexes, and red shifted for 4PANI ES and 6PANI ES except 6PANI ES-NH₃ which are due to the $\pi \rightarrow \pi^*$ transition. These value of blue and red shifts show the nPANI ES sensing ability toward CO(2), CO(1), CO₂ and NH₃. It can be said that more shifted value (but it is not true for all cases), 2PANI ES-NH₃ and 6PANI ES-NH₃ compared to other species which is totally in accordance with their difference in the value of adsorption energy.

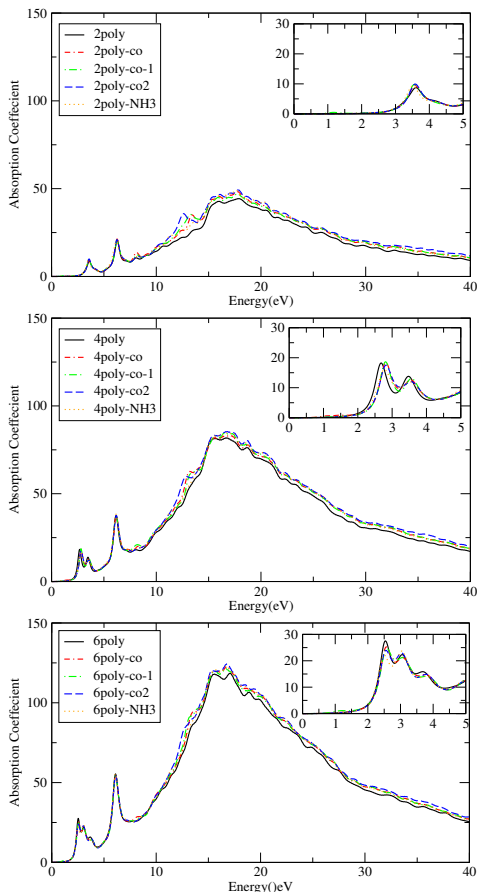


FIG. 6. Achieved absorption optical spectrum complexes and transition states corresponding to nPANIES molecule. The insets present the initial part of the spectra in a slim window.

IV. CONCLUSION

Density functional computations were carried out to study the structural, electronic, and optical properties of nPANI ES molecule and its complexes, with both QE and FHI-aims computational packages. The nearest distance between nPANI ES and gas molecules is confirmed for NH_3 by the distance around of 1.8\AA which points to strong interaction between them but $\text{CO}(1)$ and $\text{CO}(2)$ have the largest distance which points to less interaction between them. This result is completely in accordance with the obtained adsorption energies. The maximum and minimum decrease in angle $\angle \text{C}_1\text{N}_2\text{C}_3$ is about 2.07\AA and 1.1\AA in 4PANI ES- NH_3 and 6PANI ES- $\text{CO}(1)$ complexes regarding their corresponding non-complexed nPANI ES. The larger decrease in angle means the stronger electrostatic attraction between nPANI ES and NH_3 . The kind of interaction between the tested species (CO , NH_3 , CO_2) with nPANI ES is studied with an understanding of the HOMO and LUMO energies. simulating electronic features such as HL gap from the energies of HOMO and LUMO supports the sensing abil-

TABLE V. The optical absorption spectrum factor for nPANI ES and its complexes using the Liouville-lanczos approach with TD-DFT. E_F : First excited energy. λ_{max} : maximum wave length, ΔE : difference between first excited energy of nPANI ES with first excited energy of nPANI ES-X, where $X=\text{CO}(1)$, $\text{CO}(2)$, CO_2 and NH_3 .

structure	$E_F(\text{eV})$	$\lambda_{max}(\text{nm})$	$\Delta E(\text{eV})$	Result
Isolated 2PANI ES	3.60	344	-	-
2PANI ES- $\text{CO}(2)$	3.57	348	-0.02	blue
2PANI ES- $\text{CO}(1)$	3.56	348	-0.04	blue
2PANI ES- CO_2	3.59	345	-0.01	blue
2PANI ES- NH_3	3.50	353	-0.09	blue
Isolated 4PANI ES	2.67	462	-	-
4PANI ES- $\text{CO}(2)$	2.81	440	0.13	red
4PANI ES- $\text{CO}(1)$	2.81	440	0.13	red
4PANI ES- CO_2	2.81	440	0.13	red
4PANI ES- NH_3	2.77	446	0.09	red
Isolated 6PANI ES	2.54	487	-	-
6PANI ES- $\text{CO}(2)$	2.57	482	0.02	red
6PANI ES- $\text{CO}(1)$	2.58	479	0.04	red
6PANI ES- CO_2	2.55	484	0.01	red
6PANI ES- NH_3	2.50	475	-0.04	blue

ity of nPANI ES towards the above-mentioned species. The magnitude of Mulliken charge transfer is observed to be more when the adsorption of NH_3 molecule get adsorbed on nPANI ES comparing to the adsorption of other molecules. The IR spectrum of the systems with adsorption of gas molecules on an isolated nPANI ES introduce nPANI ES as a sensor. We can observe the amount of a higher and increased IR intensity in 2PANI ES- NH_3 , 4PANI ES- NH_3 and 6PANI ES- NH_3 complexes. We computed optical properties of nPANI ES molecule and its complexes using optical spectrum, next compared them with experimental. The similarity of λ_{max} and experimental λ_{max} prove the effectiveness of Liouville-Lanczos method in computing the λ_{max} and determining λ_{max} . optical absorption spectrum analysis is also applied to all species and the resulted spectra indicates that the λ_{max} were red or blue- shifted depending on the type of complex (blue-shifted for 2PANI ES and its complexes, and red shifted for 4PANI ES and 6PANI- NH_3) because of $\pi \rightarrow \pi^*$ transition which is can be considered as a testimony for the success of interaction between nPANI ES and the species tested. All analyses reveal a physisorption procedure for all species over interaction with nPANI ES.

V. ACKNOWLEDGMENTS

The authors thankfully appreciate the Sheikh Bahaei National High Performance Computing Center (SBNHPCC) for providing time and calculation facilities. SBNHPCC is supported with scientific and technological department of presidential office and Isfahan University of Technology (IUT). We want to appreciate Mr. Habib

Ullah for the fine work he did on preparing structures.

- ¹ S. Mahajan, *Pollution control in process industries* (Tata McGraw-Hill Education, 1985).
- ² B. Timmer, W. Olthuis, and A. Van den Berg, *Sensors and Actuators B: Chemical* **107**, 666 (2005).
- ³ H. Kruse and M. Tekiela, *Energy Conversion and Management* **37**, 1013 (1996).
- ⁴ S. Paul, F. Amalraj, and S. Radhakrishnan, *Synthetic Metals* **159**, 1019 (2009).
- ⁵ S. Sepaniak, T. Forges, H. Gerard, B. Foliguet, M.-C. Bene, and P. Monnier-Barbarino, *Toxicology* **223**, 54 (2006).
- ⁶ H. Bai and G. Shi, *Sensors* **7**, 267 (2007).
- ⁷ J. L. Yagüe and S. Borrós, *Plasma Processes and Polymers* **9** (2012).
- ⁸ M. Penza, G. Cassano, P. Aversa, F. Antolini, A. Cusano, A. Cutolo, M. Giordano, and L. Nicolais, *Applied Physics Letters* **85**, 2379 (2004).
- ⁹ D. Nicolas-Debarnot and F. Poncin-Epaillard, *Analytica Chimica Acta* **475**, 1 (2003).
- ¹⁰ H. Liu, J. Kameoka, D. A. Czaplewski, and H. Craighead, *Nano Letters* **4**, 671 (2004).
- ¹¹ X. Chen, C. A. Yuan, C. K. Wong, H. Ye, S. Y. Leung, and G. Zhang, *Sensors and Actuators B: Chemical* **174**, 210 (2012).
- ¹² V. Gonçalves and D. T. Balogh, *Sensors and Actuators B: Chemical* **162**, 307 (2012).
- ¹³ D. Hoa, T. S. Kumar, N. Punekar, R. Srinivasa, R. Lal, and A. Contractor, *Analytical chemistry* **64**, 2645 (1992).
- ¹⁴ S. Virji, R. B. Kaner, and B. H. Weiller, *Inorganic chemistry* **45**, 10467 (2006).
- ¹⁵ R. A. Potyrailo, C. Surman, S. Go, Y. Lee, T. Sivavec, and W. G. Morris, *Journal of Applied Physics* **106**, 124902 (2009).
- ¹⁶ N. J. Pinto, I. Ramos, R. Rojas, P.-C. Wang, and A. T. Johnson, *Sensors and Actuators B: Chemical* **129**, 621 (2008).
- ¹⁷ C. H. Choi, M. Kertesz, M.-I. Boyer, M. Cochet, S. Quillard, G. Louarn, and S. Lefrant, *Chemistry of materials* **11**, 855 (1999).
- ¹⁸ L. T. Sein, T. Duong, Y. Wei, and S. A. Jansen, *Synthetic Metals* **113**, 145 (2000).
- ¹⁹ H. Ullah, A.-u.-H. A. Shah, S. Bilal, and K. Ayub, *The Journal of Physical Chemistry C* **117**, 23701 (2013).
- ²⁰ G. Ćirić-Marjanović, *Synthetic Metals* **177**, 1 (2013).
- ²¹ S. Lim, K. Tan, E. Kang, and W. Chin, *The Journal of Chemical Physics* **112**, 10648 (2000).
- ²² A. G. MacDiarmid, *Synthetic metals* **125**, 11 (2001).
- ²³ P. Giannozzi, S. Baroni, N. Bonini, M. Calandra, R. Car, C. Cavazzoni, D. Ceresoli, G. L. Chiarotti, M. Cococcioni, I. Dabo, A. Dal Corso, S. de Gironcoli, S. Fabris, G. Fratesi, R. Gebauer, U. Gerstmann, C. Gougousis, A. Kokalj, M. Lazzeri, L. Martin-Samos, N. Marzari, F. Mauri, R. Mazzarello, S. Paolini, A. Pasquarello, L. Paulatto, C. Sbraccia, S. Scandolo, G. Sclauzero, A. P. Seitsonen, A. Smogunov, P. Umari, and R. M. Wentzcovitch, *Journal of physics. Condensed matter* **21**, 395502 (2009).
- ²⁴ V. Blum, R. Gehrke, F. Hanke, and P. Havu, *Computer Physics ...*, 1 (2009).
- ²⁵ J. P. Perdew, K. Burke, and M. Ernzerhof, *Physical review letters* **77**, 3865 (1996).
- ²⁶ M. Rocha, A. Di Santo, J. M. Arias, D. M. Gil, and A. B. Altabef, *Spectrochimica Acta Part A: Molecular and Biomolecular Spectroscopy* **136**, 635 (2015).
- ²⁷ R. G. Parr, L. v. Szentpaly, and S. Liu, *Journal of the American Chemical Society* **121**, 1922 (1999).
- ²⁸ O. B. Malcıoğlu, R. Gebauer, D. Rocca, and S. Baroni, *Computer Physics Communications* **182**, 1744 (2011).
- ²⁹ C. A. Ullrich and Z.-h. Yang, *Brazilian Journal of Physics* **44**, 154 (2014).
- ³⁰ P. K. Chattaraj and S. Giri, *Annual Reports Section "C" (Physical Chemistry)* **105**, 13 (2009).
- ³¹ A. S. Rad, *Molecular Physics* **114**, 584 (2016).
- ³² A. Al-Daghman, K. Ibrahim, N. Ahmed, and M. A. Al-Messiere, *Journal of Optoelectronics and Biomedical Materials Vol* **8**, 175 (2016).
- ³³ R. VERA A, H. ROMERO B, and E. Ahumada, *Journal of the Chilean Chemical Society* **48**, 35 (2003).